

# Structural properties of size-selected FeCo nanoparticles deposited on W(110)

Furkan Bulut · Wolfgang Rosellen · Mathias Getzlaff

Received: 28 October 2008 / Accepted: 9 April 2009 / Published online: 23 April 2009  
© Springer-Verlag 2009

**Abstract** Size-selected iron and iron–cobalt alloy clusters have been studied with high resolution transmission electron microscopy (HRTEM) and scanning tunneling microscopy (STM). The clusters were produced by a continuously working arc cluster ion source and subsequently size-selected by an electrostatic quadrupole deflector. The crystalline structure of pure clusters has been investigated with HRTEM to ensure a reliable determination of the lattice parameter for the alloy clusters. The composition of the alloy clusters was checked with energy dispersive X-ray spectroscopy (EDX). The height of the deposited FeCo clusters on the (110) surface of tungsten was determined via STM. These results were compared with the lateral size distribution being investigated by TEM and allow a conclusion on the shape of the deposited alloy clusters. Furthermore, the behavior of the alloy clusters on the W(110) surface at elevated temperatures has been examined, at which the clusters show anisotropic spreading.

**PACS** 61.46.-w · 68.37.Ef · 68.37.Og · 81.07.-b

## 1 Introduction

The physical properties of nano-sized clusters significantly differ from the corresponding bulk material. Melting point, electronic and magnetic properties of such clusters exhibit differences when compared to macroscopic material due

to decreasing coordination numbers and a high surface-to-volume ratio. A large number of surface atoms, e.g., decreases the melting point of a nanocluster to well below its known bulk value [1].

The possible applications for magnetic and electronic devices is the main motivation for a scientific interest when exploring physical properties of nanoparticles [2]. Due to the tremendous miniaturization of such devices during the last three decades this understanding has now become indispensable [3].

Furthermore, free magnetic clusters up to 700 atoms exhibit enhanced magnetic moments strongly depending on the size of the clusters [4, 5]. However, they show bulk values already at diameters above 2 nm. For clusters deposited on surfaces, on the other hand, magnetic moments can still exhibit an enhancement for sizes up to a few 10.000 atoms. The results concerning the magnetism of nanoclusters up to 12 nm can be found in [6, 7]. For a better understanding of this different behavior, it is therefore essential to investigate the structural properties of nano-sized magnetic clusters.

The shape of small clusters and their morphology after deposition on surfaces has been studied by several authors using molecular-dynamics calculations [8–11]. A detailed analysis of cluster surface interactions can be found in [12].

However, the experiments found in the literature and mentioned above were carried out with smaller clusters as the ones discussed here; the clusters deposited on W(110) surfaces exhibit sizes between 4 and 12 nm. So, several deposition experiments have been performed to characterize the clusters after landing on a hard substrate. First, it is interesting to find out whether the shape of the clusters is changing after deposition on the substrate. The question whether clusters are mobile on the W(110) surface at room and elevated temperatures and whether there exist preferential adsorption sites on the single-crystalline surface like

---

F. Bulut (✉) · W. Rosellen · M. Getzlaff  
Institut für Angewandte Physik, Universität Düsseldorf,  
Universitätsstr. 1, 40225 Düsseldorf, Germany  
e-mail: [furkan.bulut@uni-duesseldorf.de](mailto:furkan.bulut@uni-duesseldorf.de)

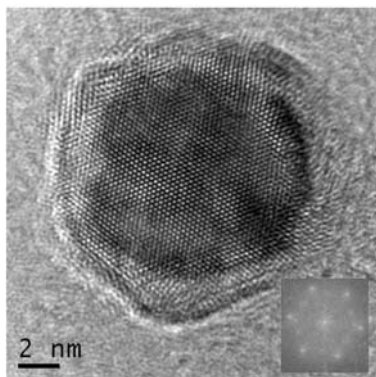


**Fig. 1** The (111) layer of an iron cluster with the corresponding FFT signal in the *inset*

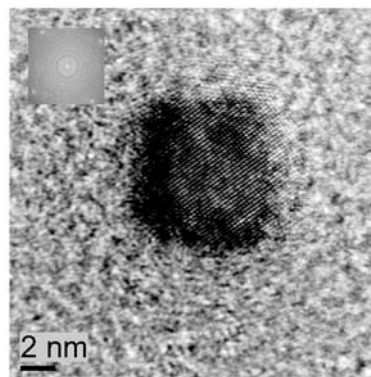


**Fig. 2** HRTEM image of an FeCo cluster exhibiting a plane in (100) orientation

step edges will also be answered. By doing so, one can determine the probability of an agglomeration of the clusters on the surface. Since the deposition takes place in the soft-landing regime, meaning that the kinetic energy per atom in a cluster is less than 0.1 eV, fragmentation of clusters after landing or damage of the surface after collision is not expected [9].

In this work, *in situ* scanning tunneling microscopy (STM) investigations concerning FeCo alloy clusters deposited on a clean W(110) surface will be presented. The clusters were formed in a hollow cathode after an arc erosion and were size selected with an electrostatic deflector prior to landing on the surface. The results were compared with high resolution transmission electron microscopy (HRTEM) images of the same clusters with respective deposition parameters. The combination of these two methods gives an idea of the shape of the clusters on the crystalline surface, since information on lateral size of the cluster cannot reliably be extracted from STM experiments. HRTEM is also a powerful tool for the determination of crystalline structure. Furthermore, the behavior of FeCo alloy clusters on W(110) at elevated temperatures has been examined.

In the next section, the experimental setup is presented. Subsequently, the results for nearly free clusters and clusters deposited on a tungsten substrate at room temperature will be discussed. Additionally, the behavior with increasing temperature is presented.

It should be mentioned that the particles reported here possess sizes of a few nanometers. Therefore, these clusters represent nanoparticles in contrary to the common sense used in the literature, where clusters are formations made up of only a few atoms.

## 2 Experimental

The preparation of the tungsten crystal, the cluster deposition experiments, and STM investigations are performed under UHV conditions. The base pressure in the entire vacuum

chamber system is well below  $5 \times 10^{-10}$  mbar. The system consists of four chambers; the first one being the cluster source connected to the quadrupole chamber. The third chamber, including the STM unit, is connected at a right angle to the quadrupole chamber and on the opposite side to the crystal preparation chamber. Only the HRTEM experiments are carried out *ex situ*, which leads to an oxide shell around the clusters. The preparation of a W(110) surface is well known in the literature [13]. The crystal is heated for about 90 minutes at 1600 K with an oxygen partial pressure of  $1 \times 10^{-6}$  mbar. In a second step, the crystal is flashed to about 2300 K to get rid of oxides. This procedure guarantees a well ordered and atomically clean W(110) surface.

The structure and cleanliness of the surface was characterized by LEED (low energy electron diffraction) and AES (auger electron spectroscopy), respectively.

The FeCo clusters are produced with a continuously working arc cluster ion source (ACIS) [14]. Due to an arc ignited between the anode and as a cathode acting target atoms are sputtered from this target at an argon pressure of 10 mbar. The metal atoms condense to clusters in the hollow cathode and undergo a supersonic expansion through an extender. Pumping stages cause the pressure to fall gradually along two skimmers until UHV conditions are reached in the quadrupole chamber.

This preparation procedure results in a large amount of charged particles. Therefore, the clusters are subsequently size-selected with an electrostatic quadrupole by deflecting them at a right angle to the sample in a last step. Assuming a uniform charge distribution and a uniform velocity, this energy filter acts as a mass filter. The deflection potential  $U_{\text{Quad}}$  varies between 250 and 1000 V. The sample is about 70 cm away from the quadrupole exit to prevent a size difference caused by the divergence of the cluster beam.

The STM used in these experiments is a MicroSPM from OMICRON. Tunneling was performed in constant current mode. The STM chamber was supported with a pneumatic vibration isolation system.

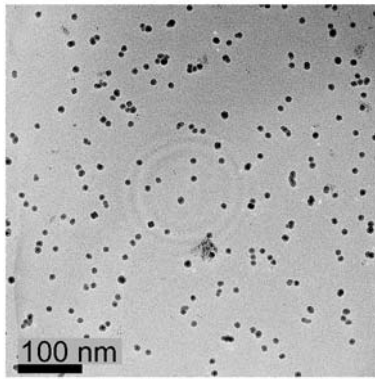


**Fig. 3**  $1.3 \mu\text{m} \times 1.3 \mu\text{m}$  TEM image of size-selected cluster with a deflection potential  $U_{\text{Quad}} = 500 \text{ V}$

The ex situ TEM experiments were performed with a Philips CM300 FEG/UT, possessing a 300 kV acceleration voltage. For the higher resolution TEM experiments, a FEI Tecnai 20T with a field emission gun operating at 200 kV was used. The TEM apparatus also enables an EDX analysis for stoichiometric investigations.

### 3 Results and discussion

#### 3.1 Crystalline structure of size-selected nearly free Fe and FeCo alloy clusters

Prior to the investigation of the crystalline properties of FeCo clusters, the lattice parameter of pure iron clusters has been determined. An investigation with a pure material concerning the reliability when determining the lattice parameter is important, since the lattice parameter of an alloy can change by varying the stoichiometry [15]. Figure 1 shows an HRTEM image of a single Fe cluster on a TEM-grid with a size of about 9 nm. According to the FFT signal, this particular image corresponds to a BCC (111) orientation. After evaluating the spots one can determine a lattice parameter of  $(0.290 \pm 0.005) \text{ nm}$  for the Fe cluster. This value is in good agreement with the theoretical value of 0.2867 nm for  $\alpha$ -iron [16]. Thus, TEM can be used as a powerful tool to determine lattice parameters for alloys with different stoichiometry, too.

For  $\text{Fe}_{1-x}\text{Co}_x$ , the alloy exhibits an ordered BCC structure (CsCl structure) up to 80% of Co, i.e., up to  $x \leq 0.8$ . Above this value, i.e., for  $x > 0.8$ , the alloy material is found in FCC structure [17]. The target material for the alloy clusters consists of  $\text{Fe}_{48}\text{Co}_{48}\text{V}_2$ . Similar results using EDX investigations for an assembly of clusters has been observed. The vanadium peak amounts to about 1% of the total amount. A  $(55 : 44) \pm 10\%$  relation for the Fe : Co composition in the alloy clusters was found. Therefore, a BCC structure is expected. The HRTEM image (see Fig. 2)

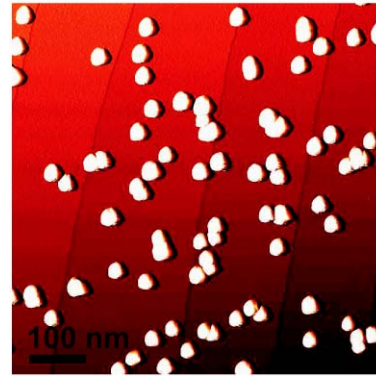


**Fig. 4**  $652 \text{ nm} \times 652 \text{ nm}$  STM image of size-selected clusters with  $U_{\text{Quad}} = 500 \text{ V}$  ( $U = 1 \text{ V}$ ,  $I = 0.1 \text{ nA}$ )

shows the (100) orientation of an FeCo cluster. Using the FFT signal a lattice parameter of  $(0.29 \pm 0.01) \text{ nm}$  with a BCC structure for these clusters was determined. This value is slightly larger than theoretical value of 0.2860 nm assuming a  $\text{Fe}_{50}\text{Co}_{50}$  composition for the target material [15, 18]. The difference between the theoretical value and the experimental one for the lattice parameter is due to the fact that the constitution of the alloy target is given for the whole material and using the EDX analysis also for an assembly of clusters, while for the high resolution TEM investigation only a single cluster is used. The constitution of this particular cluster may differ slightly from the rest of the assembly. However, this small difference does not affect the BCC structure.

HRTEM measurements also give an insight into the morphology of the nearly free clusters. Since {100} facets for FeCo clusters were observed, the morphology of the clusters corresponds to a truncated rhombic dodecahedron with 12 {110} faces and 6 {100} faces. There could also exist {111} facets like in the case of pure Fe clusters. Although this facet is energetically less favorable, especially the existence of a further truncation with additional 8 {111} facets could explain the round shape of the majority of clusters.

#### 3.2 Structure of size-selected alloy clusters deposited on W(110)

Figure 3 shows a TEM image of an assembly of FeCo clusters deposited at a deflection potential  $U_{\text{Quad}}$  of 500 V. The analysis results in a cluster diameter of  $(8.4 \pm 1.1) \text{ nm}$ . For 250 V and 1 kV one obtains  $(7.2 \pm 0.9) \text{ nm}$  and  $(10.0 \pm 1.3) \text{ nm}$ , respectively. Figure 4 presents an STM image of clusters on W(110) produced at  $U_{\text{Quad}} = 500 \text{ V}$ . The cluster heights for  $U_{\text{Quad}} = 250 \text{ V}$ , 500 V and 1 kV are  $(6.2 \pm 1.1) \text{ nm}$ ,  $(6.9 \pm 0.7) \text{ nm}$  and  $(8.4 \pm 1.1) \text{ nm}$ , respectively. Thus, the clusters exhibit a slight flattening after deposition on the tungsten substrate. This is a result of the high surface energy of W(110) compared with the cluster surface energy. The surface energy is  $4.005 \text{ J/m}^2$  for this particular

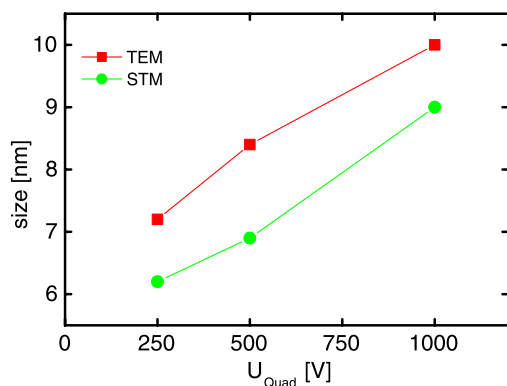


**Fig. 5** Comparison between the lateral size of size-selected clusters (TEM) and the height of clusters on W(110) (STM) for different cluster sizes indicating a size reduction of about 1 nm

surface of tungsten [19]. Furthermore, the oblate structure is caused by surface atoms of the cluster that diffuse on to the tungsten surface, where they become almost immobile. A high mobility for surface atoms of a  $\text{Fe}_{586}$  cluster has been calculated, e.g., by Ding et al. [20]. A flattening caused by cluster surface collision can be neglected. Since the kinetic energy of the clusters is about 1 keV and the clusters consist of a few 10,000 atoms, the clusters are deposited under soft landing conditions with a deposition energy well below 0.1 eV/atom. The decrease in the height of the size-selected clusters on W(110) is about 1 nm (see Fig. 5). Figure 6 is an example for the STM (height of clusters) and TEM (lateral size of clusters) experiments using a quadrupole potential of about 500 V.

The STM image (see Fig. 4) additionally proves that the clusters are arbitrarily located on the W(110) surface. They do not prefer step edges or any other energetically favorable sites. The mobility of the clusters on W(110) is too low at room temperature to cause any agglomeration on the surface. The accumulation of the clusters at particular sites is a result of cluster assembling at the same site during the deposition process and does not represent the coalescence of clusters after diffusion on the surface.

### 3.3 Melting of FeCo clusters on W(110) at elevated temperatures

The tungsten crystal with the deposited FeCo alloy clusters was resistively heated on a manipulator at 573, 923, 1023, and 1123 K.

At 573 K, no significant change concerning the distribution of the height as well as shape of the clusters was observed.

At 923 K, the height of the clusters decreased from about 7 nm ( $U_{\text{Quad}} = 500$  V) to 4 nm, indicating a melting of the clusters on the surface.

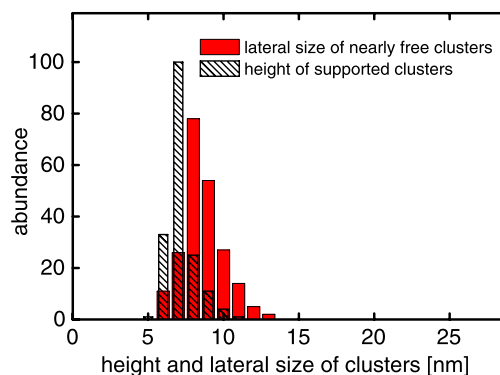


**Fig. 6** Comparison between the lateral size of size-selected clusters (TEM) and the height of clusters on W(110) (STM) for  $U_{\text{Quad}} = 500$  V

A direct observation of the melting could be observed at a high temperature of 1023 K, at which most of the clusters show anisotropic melting. In order to melt all the clusters observably on the surface, the temperature was raised to 1123 K. Figure 7 shows an STM image of clusters after a temperature treatment at 1123 K for 1 hour. It is obvious that the melting takes place anisotropically along the [001] direction of the W(110) surface.

The diffusion of adsorbed Fe and Co atoms on W(110) and the anisotropic spreading of iron and cobalt islands on W(110) was already reported in the literature. According to [22], the diffusion of single atoms on the W(110) surface occurs along the  $[\bar{1}11]$  direction. Simultaneous hoppings can result in motion either in the  $[1\bar{1}0]$  or in the [001] direction with the same activation energy, resulting in a different spreading along these axes. Iron, e.g., elongates in the  $[1\bar{1}0]$  direction whereas the spreading of cobalt is site dependent on W(110) as reported by [21].

The reason why the FeCo clusters deposited on W(110) in this present work mainly melt along the [001] axis on the contrary to the work of Reuter et al. [21] is not clear. One reason could be the presence of cobalt which has a different melting behavior than iron. Another explanation could be the size of the cluster. The iron or cobalt islands discussed in the literature mentioned above deal with the spreading of iron dots which are much bigger than the clusters here. The unrolling carpet mechanism which defines the spreading of an iron dot on W(110) [21], where atoms roll down to the surface and form a monolayer by hopping over already unrolled part of the island, may not be the dominant process in cluster melting. Thus, this point will be investigated in the future with experiments carried out on melting of pure iron and pure cobalt clusters on W(110).

## 4 Conclusion

Magnetic iron–cobalt alloy nanoparticles were studied with high resolution transmission electron microscopy (HRTEM)

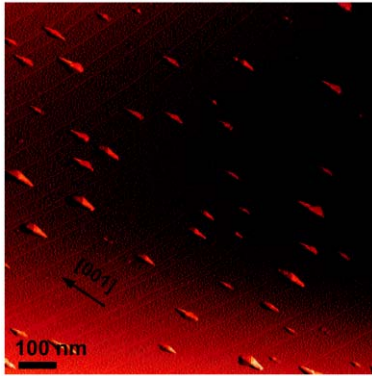


**Fig. 7** The melting of FeCo clusters along the [001] direction on W(110) after heating for 1 hour at 1123 K ( $U = 1$  V,  $I = 0.1$  nA)

and scanning tunneling microscopy (STM). The nanoparticles were produced with a continuously working arc cluster ion source and subsequently size-selected with an electrostatic quadrupole deflector.

The composition of the alloy nanoparticles was checked with energy dispersive X-ray spectroscopy (EDX). The composition of the alloy nanoparticles was in good agreement with the target material.

The lateral size distribution was investigated by TEM and the height of the deposited FeCo nanoparticles on the (110) surface of tungsten was determined by STM. Comparing the results it is obvious that the nanoparticles deposited on W(110) were flattened due to a significant cluster-surface interaction.

The crystalline structure of pure nanoparticles has also been investigated with HRTEM to ensure a reliable determination of the lattice parameter for the alloy nanoparticles. For Fe nanoparticles, the lattice parameter agrees well with the theoretical values. HRTEM investigations have shown that the FeCo nanoparticles have a truncated rhombic dodecahedral shape with a CsCl structure. Using the FFT signal from the HRTEM image a lattice constant of about 0.29 nm for the FeCo nanoparticles was determined.

**Acknowledgements** We wish to thank Wilfried Assenmacher (University of Bonn, AG Mader), Daniela Sudfeld and Marina Spasova

(University of Duisburg-Essen, AG Farle) for the HRTEM and EDX analysis. We gratefully acknowledge the financial support of the Deutsche Forschungsgemeinschaft (DFG) within the priority program 1153 ‘clusters in contact with surfaces’.

## References

1. I. Shyjumon, M. Gopinadhan, O. Ivanova, M. Quaas, H. Wulff, C.A. Helm, R. Hippler, *Eur. Phys. J. D* **37**, 409 (2006)
2. J.P. Pierce, E.W. Plummer, J. Shen, *Appl. Phys. Lett.* **81**, 1890 (2002)
3. W.A. de Heer, *Rev. Mod. Phys.* **65**, 611 (1993)
4. J.P. Bucher, L.A. Bloomfield, *Int. J. Mod. Phys. B* **7**, 1079 (1993)
5. I.M.L. Billas, J.A. Becker, A. Châtelain, W.A. de Heer, *Phys. Rev. Lett.* **71**, 4067 (1993)
6. J. Bansmann, A. Kleibert, *Appl. Phys. A* **80**, 957 (2005)
7. J. Bansmann, S.H. Baker, C. Binns, J.A. Blackman, J.-P. Bucher, J. Dorantes-Dávila, V. Dupuis, L. Favre, D. Kechrakos, A. Kleibert, K.-H. Meiwes-Broer, G.M. Pastor, A. Perez, O. Toulemonde, K.N. Trohidou, J. Tuaille, Y. Xie, *Surf. Sci. Rep.* **56**, 189 (2005)
8. H. Haberland, Z. Insepov, M. Kurrais, M. Mall, M. Moseler, Y. Thurner, *Nucl. Instrum. Methods Phys. Res. B* **80/81**, 1320 (1993)
9. H. Haberland, Z. Insepov, M. Moseler, *Phys. Rev. B* **51**, 11061 (1995)
10. G. Betz, W. Husinsky, *Nucl. Instrum. Methods Phys. Res. B* **122**, 311 (1997)
11. H. Hsieh, R.S. Averback, H. Sellers, C.P. Flynn, *Phys. Rev. B* **45**, 4417 (1997)
12. K.-H. Meiwes-Broer, *Metal Clusters at Surfaces* (Springer, Berlin, 2000)
13. R.W. Joyner, J. Rickman, M.W. Roberts, *Surf. Sci.* **39**, 445 (1973)
14. R.-P. Methling, V. Senz, E.-D. Klinkenberg, Th. Diederich, J. Tiggesbäumker, G. Holzhüter, J. Bansmann, K.H. Meiwes-Broer, *Eur. Phys. J. D* **16**, 173 (2001)
15. W.B. Pearson, *Handbook of Lattice Spacings & Structures of Metals and Alloys*. International Series of Monographs on Metal Physics and Physical Metallurgy, vol. 4 (Pergamon, New York, 1958)
16. D.E. Grey, *American Institute of Physics Handbook* (McGraw-Hill, New York, 1972)
17. M.R. Andrews, *Phys. Rev.* **18**, 245 (1921)
18. H. Moumeni, S. Alleg, C. Djebbari, F.Z. Bentayeb, J.M. Grenche, *J. Mater. Sci.* **39**, 5441 (2004)
19. L. Vitos, A.V. Ruban, H.L. Skriver, J. Kollár, *Surf. Sci.* **411**, 186 (1998)
20. F. Ding, K. Bolton, A. Rosén, *Eur. Phys. J. D* **34**, 275 (2005)
21. D. Reuter, G. Gerth, J. Kirschner, *Phys. Rev. B* **57**, 2520 (1997)
22. D. Spišák, J. Hafner, *Surf. Sci.* **584**, 55 (2005)